

Impact of Ozone Post Oxidation to the Electrical Properties of HfO₂/Al₂O₃/GeO_x/Ge pMOSFETs

¹Rui Zhang, ¹Xiaoyu Tang, ¹Xiao Yu, ¹Junkang Li and ^{1,2}Yi Zhao*

¹College of Electronic Engineering and Information Science, Zhejiang University, Hangzhou 310027, China.

²State Key Laboratory of Silicon Materials, Zhejiang University, Hangzhou 310027, China

*E-mail: yizhao@zju.edu.cn

Introduction

Ge has been regarded as a promising channel material of MOSFETs for further improving the Si CMOS performance, especially for the pMOSFET applications, because of its high bulk hole mobility [1-3]. It is mandatory to fabricate a superior high-*k*/Ge gate stack with low D_{it} and thin EOT simultaneously to obtain high performance Ge pMOSFETs [4]. A plasma post oxidation (PPO) method has been developed by using oxygen plasma to oxidize the high-*k*/Ge interface to fabricate HfO₂/Al₂O₃/GeO_x/Ge gate stacks with low D_{it} of 10^{11} cm²eV⁻¹ and thin EOT of 0.76 nm, yielding high mobility (546 cm²/Vs) (100) Ge pMOSFETs [5, 6]. However, a further reduction of EOT is not easy for the PPO HfO₂/Al₂O₃/GeO_x/Ge pMOSFETs, since the mobility degrades with reducing the EOT. In this study, an ozone post oxidation (OPO) method is purposed by using an *in-situ* ozone annealing of ALD HfO₂/Al₂O₃/Ge structures, featuring a low D_{it} at 10^{11} cm²eV⁻¹ level and an ultrathin EOT of 0.6 nm. As a result, the high mobility (100) Ge pMOSFETs using these gate stacks have been realized with an ultrathin EOT of 0.6 nm.

Experimental

The fabrication process of OPO HfO₂/Al₂O₃/GeO_x/Ge gate stacks is shown in Fig. 1. After pre-cleaning of the Ge substrates, the HfO₂ (2 nm)/Al₂O₃ (0.3 nm) structures were deposited by ALD at 300 °C. After that, the *in-situ* OPO was carried out at 300 °C in the ALD chamber. The PDA was preformed for the gate stacks at 400 °C in N₂ ambient for 30 min.

In order to evaluate the impact of OPO to electrical properties of the OPO HfO₂/Al₂O₃/GeO_x/Ge gate stacks, MOS capacitors were fabricated with Au as gate metal. The Ge pMOSFETs with the OPO HfO₂/Al₂O₃/GeO_x/Ge gate stacks were also fabricated with a conventional gate last process. After the S/D formation by B ion implantation (10 keV, 10^{15} cm⁻²) and dopant activation annealing, the TiN/HfO₂/Al₂O₃/GeO_x/Ge gate stacks were deposited with different OPO times. Finally, the Ni contact pads were deposited for gate and S/D by the thermal evaporation.

Results and discussion

Fig. 2 shows the angle-resolved XPS spectra taken from an HfO₂ (2 nm)/Al₂O₃ (0.3 nm) structure after 15 s' OPO. In contrast to the HfO₂ peak intensity, the intensity of GeO_x peak reduces with a decrease of take-off angle. This phenomenon indicates that the GeO_x IL is formed underneath the HfO₂ layer. On the other hand, the thickness of GeO_x IL is increased with elongating the OPO time (Fig. 3). The detailed structure of the OPO HfO₂/Al₂O₃/GeO_x/Ge gate stack was investigated by TEM (Fig. 4). The thickness of IL is 0.7 nm after 60 s' OPO, corresponding to the 0.3-nm-thick Al₂O₃ layer and

a formation of 0.4-nm-thick GeO_x layer. The superior C-V characteristics have been observed in the OPO Au/HfO₂/Al₂O₃/GeO_x/Ge MOS capacitor, thanks to the passivation of D_{it} in the gate stacks (Figs. 5 and 6). The EOT of the Au/HfO₂/Al₂O₃/GeO_x/Ge MOS capacitor is 0.6 nm. It is interestingly noted that the EOT of the OPO MOS capacitor is even thinner than that of the MOS capacitor without OPO (0.82 nm) (Fig. 7). The decreased EOT of the gate stacks after OPO is attributable to the crystallization of HfO₂, which leads to the increase of HfO₂ permittivity [7] and compromises the EOT increase caused by GeO_x IL formation. This phenomenon is also confirmed by measuring the permittivity of HfO₂ by using the HfO₂ (5 nm)/Al₂O₃ (1 nm)/Ge structures with ozone annealing for different times (Fig. 8).

The (100)/<110> HfO₂/Al₂O₃/GeO_x/Ge pMOSFETs were fabricated with different OPO times. Figs. 9 and 10 show the I_d - V_d and I_d - V_g characteristics of the HfO₂/Al₂O₃/GeO_x/Ge pMOSFET with 60 s' OPO, with an ultrathin EOT of 0.6 nm. The normal operations have also been confirmed for the HfO₂/Ge and the HfO₂/Al₂O₃/Ge pMOSFETs. The HfO₂/Al₂O₃/GeO_x/Ge pMOSFET exhibits an S factor of 85 mV/dec, corresponding to a D_{it} of 2.3×10^{12} cm²eV⁻¹ and agrees with the D_{it} measurement results in Fig. 6. The effective hole mobility of these Ge pMOSFETs were evaluated by using the split C-V method (Fig. 11). The improved mobility is observed for the devices with longer OPO times, due to the D_{it} reduction in the gate stack. Especially, the peak hole mobility of 417 cm²/Vs has been achieved for the HfO₂/Al₂O₃/GeO_x/Ge pMOSFETs with 0.6 nm EOT. As shown in the benchmark of the peak mobility in high-*k*/Ge pMOSFETs, the record high peak mobility is obtained for the OPO HfO₂/Al₂O₃/GeO_x/Ge pMOSFETs with EOT of 0.6 nm.

Conclusion

The ultrathin EOT and low D_{it} HfO₂/Al₂O₃/GeO_x/Ge gate stacks with superior electrical properties have been fabricated by using the ozone post oxidation method, featuring the crystallization of HfO₂ and the GeO_x IL formation simultaneously. As a result, high mobility (417 cm²/Vs) Ge pMOSFETs have been realized with an ultrathin EOT of 0.6 nm.

Acknowledgement This work was supported by National Natural Science Foundation of China (No. 61306097 and No. 61376097).

Reference [1] S. Takagi, et al., *IEDM*, pp. 57, 2003. [2] H. Shang, et al., *IBM J. Res. Dev.*, vol. 50, pp. 377, 2006. [3] K. C. Saraswat, et al., *Microelectron. Eng.*, vol. 80, pp. 15, 2005. [4] A. Toriumi, et al., *Microelectron. Eng.*, vol. 86, pp. 2314, 2007. [5] R. Zhang, et al., *IEDM*, pp. 59, pp. 335, 2012. [6] R. Zhang, et al., *IEDM*, vol. 60, pp. 927, 2013. [7] S. Migita, et al., *VLSI*, pp. 119, 2008.

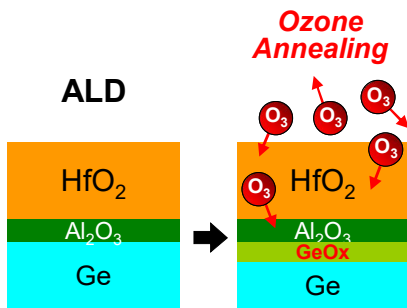


Fig. 1 Fabrication process flow of the HfO₂/Al₂O₃/GeO_x/Ge gate stacks by ozone post oxidation (OPO).

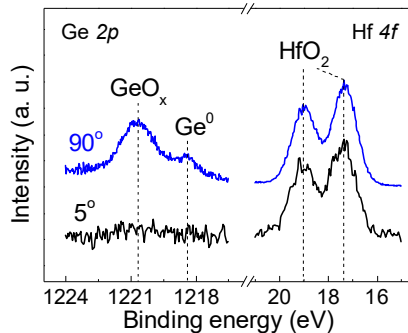


Fig. 2 The AR-XPS spectra taken from a HfO₂ (2 nm)/Al₂O₃ (0.3 nm)/Ge structure with OPO for 15 s at 300 °C.

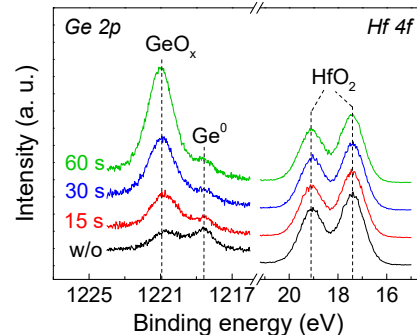


Fig. 3 The XPS spectra taken from a HfO₂ (2 nm)/Al₂O₃ (0.3 nm)/Ge structure w/o and w/ OPO for different times.

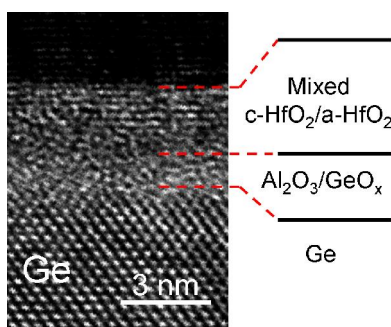


Fig. 4 The cross section TEM image of the OPO HfO₂/Al₂O₃/GeO_x/Ge gate stack with a 60 s' OPO.

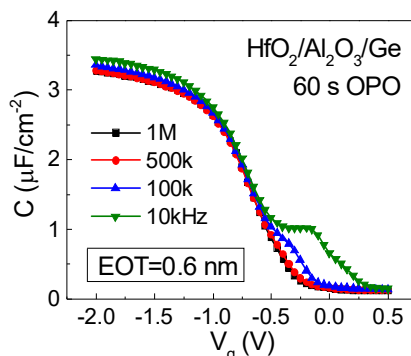


Fig. 5 The C-V characteristics of an Au/HfO₂/Al₂O₃/GeO_x/Ge MOS capacitor with a 60 s' OPO.

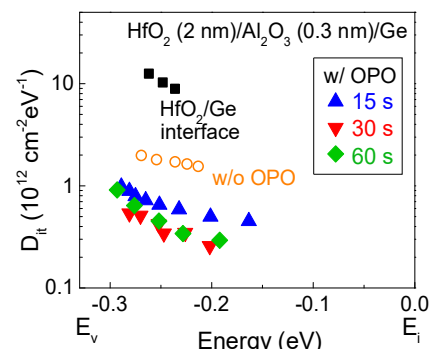


Fig. 6 The energy distribution of D_{it} in the Au/HfO₂/Al₂O₃/GeO_x/Ge MOS capacitors with different OPO times.

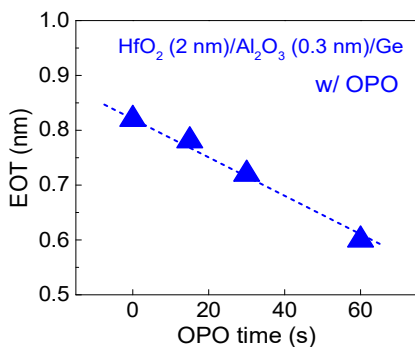


Fig. 7 The EOT of the OPO HfO₂/Al₂O₃/GeO_x/Ge gate stacks with different OPO times.

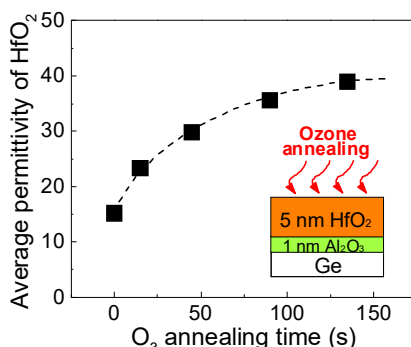


Fig. 8 The permittivity of HfO₂ after the ozone annealing for different times.

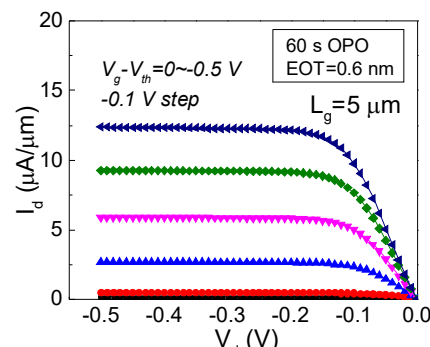


Fig. 9 The I_d-V_d characteristics of the Ge pMOSFET with the HfO₂/Al₂O₃/GeO_x/Ge gate stack having a 60 s' OPO.

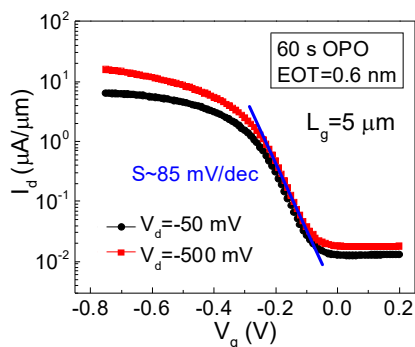


Fig. 10 The I_d-V_g characteristics of the Ge pMOSFET with the HfO₂/Al₂O₃/GeO_x/Ge gate stack having a 60 s' OPO.

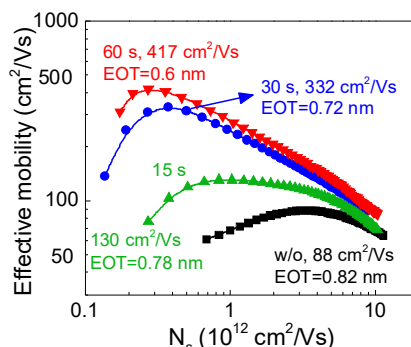


Fig. 11 The effective hole mobility of the Ge pMOSFETs with the HfO₂/Al₂O₃/GeO_x/Ge gate stacks having different OPO times.

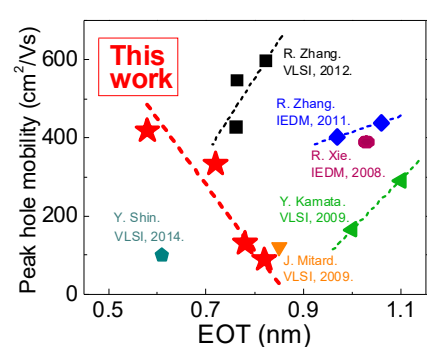


Fig. 12 The benchmarking of peak hole mobility in Ge pMOSFETs with ultrathin EOT gate stacks.